Overcoming limitations of passive invisible antennas through bianisotropic nonreciprocal mantle cloaks

Zahra Hamzavi-Zarghani,[1] Alessio Monti[ORCID],[1,*] Stefano Vellucci,[2] Mirko Barbuto,[2] Michela Longhi,[2] Davide Ramaccia,[1] Luca Stefanini[ORCID],[1] Alessandro Toscano,[1] and Filiberto Bilotti[1]

[1]*Department of Industrial, Electronic and Mechanical Engineering, Roma Tre University, Via Vito Volterra 62, 00146, Rome, Italy*

[2]*Department of Engineering, Niccolò Cusano University, Via don Carlo Gnocchi 3, 00166, Rome, Italy*

This paper explores the use of bianisotropic mantle cloaks to reduce the scattering of a dipole antenna at its own operation frequency, preserving the radiating properties in transmission mode. The proposed model is based on the use of generalized sheet transition conditions to derive the susceptibilities that make the metasurface operate as a nonreciprocal transparent cloak characterized by zero scattering for external illumination and full transmission for antenna radiation. The ideal metasurface cloak is then implemented through an active metasurface integrating transistors acting as isolators. Simulation results confirm the proper behavior of the cloaked antenna, which exhibits excellent radiation performances in transmission mode and a low-scattering cross section in receiving mode.

I. INTRODUCTION

Antenna technology plays a central role in the development of wireless communication and sensing systems. The rapid growth of high-density integrated wireless systems leads to an increasing number of antennas existing on the same platform, operating in either overlapping or separated frequency channels. At the same time, however, ever more dense antenna systems introduce degradation of electrical and radiating performances of the antennas, due to unavoidable mutual coupling and blockage effects [1–3].

Cloaking or invisibility devices, based on different approaches, including transformation optics [4,5], transmission lines [6–8], and scattering cancellation [9–13], were recently used to overcome the mentioned limitations of supercrowded platforms. Cloaking devices, in fact, can be wrapped around antennas to reduce their scattering response, thus reducing blockage effects and mutual coupling [5,14–16] in a system consisting of two closely spaced antennas, which can individually operate, as if they were alone in the platform. Several designs and experimental results based on the use of the mantle cloaking approach have been reported for linear [14–16], strip [17], and printed antennas [18], as well as for antenna arrays [19,20].

Similar results can also be achieved by replacing conventional antennas with properly designed cloaks exhibiting a low-scattering cross section over a desired frequency range, while behaving as efficient radiators in another one. In Ref. [8], this solution was explored for transmission-line cloaks. Several straightforward geometric modifications can transform a regular transmission-line cloak into a dipole or monopole antenna. A similar device was also designed in Ref. [3], using an inductive metasurface surrounding a dielectric core. In this case, the design takes advantage of the intrinsically low-scattering nature of subwavelength dielectric objects and of the strong frequency-dispersive behavior of inductive metasurfaces.

Regardless of the specific technique used to achieve the invisibility effect, in all the previously mentioned works, the cloaks consist of linear, passive, and reciprocal structures. It has been widely demonstrated that this kind of cloak can be used to effectively reduce *only the out-of-band scattering of an antenna*. As a consequence of the optical theorem [21–23], in fact, any passive, linear, and reciprocal cloak would unavoidably affect the radiative performances of the antenna if used to reduce scattering at its own operating (i.e., resonance) frequency. In other words, all the structures discussed in Refs. [1–20,24–26] lack the fundamental capability to effectively cloak antennas at their designated operational frequencies without adversely affecting their radiation performance. This limitation stems from the constraints of passive cloaking, as outlined in the optical theorem. In Ref. [27], this phenomenon was elucidated by focusing on linear antennas. Specifically, it was shown that, when the antenna was cloaked at its own resonance frequency, the resulting realized-gain pattern experienced a significant deterioration in comparison to the uncloaked

*Corresponding author: alessio.monti@uniroma3.it

064045-1

case. The degradation is due to the impedance mismatch between the antenna and its feed, which is induced by the cloaking device that modifies the antenna input impedance to satisfy the optical theorem. This fundamental limitation, which is a consequence of antenna reciprocity, cannot be overcome by using passive, linear, and reciprocal cloaks. Nonetheless, in some specific scenarios, characterized by different power levels or waveforms of the signals emitted and received by the antennas, it can be circumvented by using simple circuit-loaded metasurfaces. In Refs. [27,28], for instance, it was shown that diode-loaded metasurfaces allowed independent control of the scattering and radiation patterns of antennas, as long as the power levels of the received and transmitted signals were significantly different. Similar results were also obtained in Ref. [29], considering signals with different waveforms. Although the method proposed in Refs. [27–29] mitigates the passive cloak's limitations through the integration of nonlinear concepts, adjustment of the power level for internal and external fields can be a challenging task and, above all, is not always possible in application scenarios.

In recent years, efforts have been devoted to overcoming the constraints associated with linear, passive, and reciprocal cloaking devices. For instance, the use of active non-Foster circuits has been suggested as a way to significantly expand the operative bandwidth of mantle cloaks [30]. Additionally, the distinctive characteristics of parity-time symmetric structures have been suggested as a potential avenue to offset losses, enabling the creation of genuinely invisible sensors, demonstrating unidirectional cloaking [31,32]. Remarkably, in a recent publication [33], a transmissive bianisotropic cloak design was introduced. Such a cloak exhibits a nonreciprocal transmissive characteristic and is able to make a linear antenna invisible at a desired frequency, while retaining its radiation efficiency and impedance matching with the source in the same frequency range. However, the designed cloak consists of multilayered metasurfaces, resulting in a bulky and complex structure.

Inspired by this recent development, our work explores the design of a single-layer bianisotropic nonreciprocal mantle cloak for dipole antennas. This cloak has the capability to reduce the power scattered by the antenna while maintaining satisfactory radiation properties at the same frequency. In addition, given its simple single-layer geometry, it can be easily implemented through an active metasurface layout, as discussed and optimized in this paper. Notably, the structure proposed herein represents a pioneering advancement as a single-layer bianisotropic nonreciprocal mantle cloak.

The transition from a multilayered to a single-layered cloak directly stems from the different cloaking scheme exploited here, the so-called mantle cloaking approach, which is particularly applicable to electrically small cylinders, such as wire antennas. The cloaking approach

exploited in Ref. [33], defined by the authors as a "metasurface-enhanced Fabry-Perot resonator," requires multiple layers to achieve the reduction in scattering for external illumination. Conversely, here, we exploit the principle of the cancellation of scattering by the currents induced in the metasurface for external illumination. This approach streamlines the cloak design and implementation, provided that the size of the object to hide is subwavelength. The significance of adopting a single-layer design for active devices cannot be understated, as it offers tangible benefits, in terms of cost reduction, system stability, and facilitating the feeding of the structure. In fact, in contrast to Ref. [33], here, we also propose a realistic implementation of such a nonreciprocal cloak.

The paper is structured as follows. Section II presents the modeling of a bianisotropic metasurface, employing generalized sheet transition conditions (GSTCs) based on electric and magnetic susceptibilities. This section also discusses a strategy for its numerical modeling, based on the use of effective electric and magnetic surface currents. Then, a two-step design procedure for the cloak is proposed. In the first step, the transmission regime of the cloaked antenna under the assumption of a zero external field is considered, allowing the derivation of the design criteria for some of the susceptibilities of the bianisotropic cloaking metasurface. In the second step, the behavior of the cloaked antenna is analyzed when illuminated by an external field, introducing further conditions for metasurface susceptibilities. Section III is focused on the numerical validation of the proposed design approach and on the refinement of the cloak design to account for the finite size of the cloaked antenna. Finally, in Sec. IV, a possible realistic design of the optimized nonreciprocal bianisotropic cloak is proposed, based on an active metasurface layout. Full-wave simulation results are also reported to confirm the expected operation of the cloaked antenna.

II. MODELING AND SYNTHESIS OF THE BIANISOTROPIC NONRECIPROCAL CLOAK

The structure under investigation is shown in Fig. 1 and consists of a linear half-wavelength dipole surrounded by a bianisotropic sheet (hereafter referred to as the *transparent mantle cloak*). As discussed above, the cloak should be designed to exhibit transparent behavior when the antenna is transmitting (*transmission scenario*) and partially reflective behavior when the antenna is illuminated by an external plane wave (*external illumination scenario*). The transparent behavior is required to allow the antenna to work properly in transmission mode, while the partially reflective behavior is needed to achieve scattering cancellation for external illumination.

In this section, we first describe how to model a bianisotropic metasurface through GSTCs. Then, we derive a
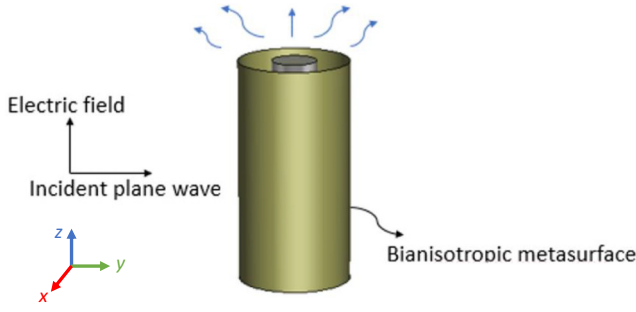
FIG. 1. Half-wavelength dipole surrounded by a bianisotropic transparent cloak. Cloak is designed to exhibit transparent behavior when the antenna operates in transmitting mode and to cancel out antenna scattering when the radiator is illuminated by an external plane wave.

synthesis approach for the cloak by discussing the transmission and external illumination scenarios separately, with the aim of deriving the required conditions for the susceptibilities of the bianisotropic sheet.

A. Modeling of a bianisotropic metasurface

A bianisotropic metasurface can be effectively represented through the use of GSTCs, which offer a comprehensive extension of the classical boundary conditions, incorporating bianisotropic surface-polarization current densities [34–38]. Assuming an $e^{j\omega t}$ time dependence, GSTCs in cylindrical coordinates for a transverse magnetic (TM$_z$) polarized plane wave are read as

$$H_\varphi^2 - H_\varphi^1|_{\rho=a_c} = \frac{jk_0}{\eta_0}(\chi_{ee}^{zz}E_{z,av} + \eta_0\chi_{em}^{z\varphi}H_{\varphi,av}),$$
$$E_z^2 - E_z^1|_{\rho=a_c} = jk_0(\chi_{me}^{\varphi z}E_{z,av} + \eta_0\chi_{mm}^{\varphi\varphi}H_{\varphi,av}), \tag{1}$$

where a_c is the radius of the cylindrical metasurface and superscripts 1 and 2 refer to the outside and inside of the metasurface, respectively; $E_{z,av}$ and $H_{\varphi,av}$ correspond to the average z and φ components of the electric and magnetic fields, respectively; k_0 and η_0 are the free-space wave number and wave impedance, respectively. Finally, χ_{ee}^{zz}, $\chi_{em}^{z\varphi}$, $\chi_{me}^{\varphi z}$, and χ_{mm}^{zz} are the electric to electric, magnetic to electric, electric to magnetic, and magnetic to magnetic susceptibilities of the bianisotropic metasurface, respectively. The reciprocity principle imposes that $\chi_{em}^{z\varphi} = -\chi_{me}^{\varphi z}$, whereas, in the absence of gain and loss, the condition implies that χ_{ee}^{zz} and χ_{mm}^{zz} are entirely real, while $\chi_{em}^{z\varphi} = -\chi_{me}^{\varphi z}$ are purely imaginary [33–35].

According to Eq. (1), when a TM$_z$-polarized incident wave interacts with a bianisotropic metasurface, it induces discontinuities in both tangential electric and magnetic fields. These discontinuities give rise to the excitation of an electric surface current in the z direction ($J_{es,z}$) and a magnetic surface current in the φ direction ($J_{ms,\varphi}$). Therefore, a bianisotropic metasurface can be modeled through

the following surface currents [39]:

$$J_{es,z} = H_\varphi^2 - H_\varphi^1|_{\rho=a_c},$$
$$J_{ms,\varphi} = E_z^2 - E_z^1|_{\rho=a_c}. \tag{2}$$

Equation (2) is used in Sec. IV to model the bianisotropic sheet in full-wave simulations and to check the theoretical results.

B. Synthesis of the transparent cloak: Transmission scenario

To investigate transmission mode, we assume the absence of an external field (i.e., the incidence plane wave shown in Fig. 1) and that the antenna is excited through a wave port placed between its two arms. If the metasurface, working as a cloaking structure, is placed sufficiently far from the dipole, the wave impinging onto the metasurface can be approximated as a plane wave. Consequently, to achieve perfect transmission from the antenna to free space, the following conditions, regarding the fields on either side of the metasurface, must be satisfied [33]:

$$E_z^2 = E_z^1 = 1,$$
$$H_\varphi^2 = H_\varphi^1 = -\frac{1}{\eta_0}. \tag{3}$$

Substituting Eq. (3) into Eq. (1) leads to a pair of relationships between susceptibilities:

$$\chi_{ee}^{zz} = \chi_{em}^{z\varphi},$$
$$\chi_{me}^{\varphi z} = \chi_{mm}^{\varphi\varphi}. \tag{4}$$

Equation (4) represent the first two conditions that the bianisotropic metasurface should satisfy to behave as a transparent mantle cloak.

C. Synthesis of the transparent cloak: External illumination scenario

In the context of external illumination, we investigate the interaction between an infinitely long metal cylinder and a TM$_z$-polarized incident wave. The electric fields associated with the incident and scattered waves, denoted as E_i and E_s, respectively, and the electric field in the region between the metal cylinder and the metasurface named as E_{in} can be expanded into cylindrical harmonics, as follows [40]:

$$E_i = \hat{z}E_0 \sum_{n=-\infty}^{\infty} j^{-n}J_n(k_0\rho)e^{jn\varphi}, \tag{5}$$

$$E_{in} = \hat{z}E_0 \sum_{n=-\infty}^{\infty} j^{-n}(a_nJ_n(k_0\rho) + b_nY_n(k_0\rho))e^{jn\varphi}, \tag{6}$$

$$E_s = \hat{z}E_0 \sum_{n=-\infty}^{\infty} j^{-n}c_nH_n^2(k_0\rho)e^{jn\varphi}, \tag{7}$$

where J_n, Y_n, and H_n^2 represent the Bessel functions of the first and second kind and the Hankel function of the second kind, respectively. Magnetic fields can be determined by applying Maxwell's equations in conjunction with the electric fields described in Eqs. (5)–(7). The unknown coefficients a_n, b_n, and c_n can be derived by imposing boundary conditions $E_z = 0$ on the antenna surface and the GSTCs ones on the metasurface expressed by Eq. (1).

Under the assumption of an electrically small radius of the cloak, we can neglect higher harmonics and focus on the fundamental scattering [i.e., limit the sum in Eqs. (5)–(7) to the $n = 0$ order] [41,42]. Applying the scattering-cancellation technique, we impose that the first harmonic of the scattered wave is equal to zero (i.e., $c_0 = 0$) [43] and obtain the following relationship between $\chi_{em}{}^{z\varphi}$ and $\chi_{me}{}^{\varphi z}$:

$$\chi_{ee} = \frac{[m(1 - j\,0.5k_0\chi_{me})Y_1(a_c k_0)]J_0(k_0 a_c) + j\,k_0\chi_{me}J_1(k_0 a_c)}{k\{J_0(k_0 a_c)[-j\,0.5mY_1(k_0 a_c) + j\,J_1(k_0 a_c) - mY_0(k_0 a_c)] - j\,0.5mJ_1(k_0 a_c)Y_0(k_0 a_c) + J_0^2(k_0 a_c)\}}$$
$$+ \frac{[-k_0\chi_{me}J_1(k_0 a_c) + m(k_0\chi_{me}Y_1(k_0 a_c) - (1 + j\,0.5k_0\chi_{me})Y_0(k_0 a_c))]J_1(k_0 a_c)}{k\{J_0(k_0 a_c)[-j\,0.5mY_1(k_0 a_c) + j\,J_1(k_0 a_c) - mY_0(k_0 a_c)] - j\,0.5mJ_1(k_0 a_c)Y_0(k_0 a_c) + J_0^2(k_0 a_c)\}},$$

$$(8)$$

with

$$m = \frac{\pi}{2Ln[1.78k_0 a/2]}.$$

Combining Eq. (8) with the conditions of Eq. (4) obtained in transmission mode returns the requirements for the transparent mantle cloak.

It is worth recalling that, in the transmission scenario, we use an approximation that only holds when the radius of the cloak is large enough to ensure that the field radiated by the antenna and impinging onto the metasurface is approximately a plane wave. In this section, instead, we focus on cloaks with electrically small radii, such that the higher-order scattering harmonics can be neglected. Therefore, it should be clear that a trade-off between these two requirements will be needed to achieve a final working design.

Furthermore, it should be emphasized that the scattering-cancellation technique discussed in this section has been developed for infinitely long metal cylinders and not for half-wavelength dipoles. Therefore, the susceptibility values obtained through this analysis only represent an initial guess to be refined through numerical simulations. To calculate the scattering width of the cloaked cylinder with infinite length, we apply [40,44]

$$\sigma_{2D} = \frac{4}{k_0} \sum_{n=-\infty}^{\infty} |c_n|^2,$$

$$(9)$$

and to determine the RCS of the cloaked antenna with a finite length of h, the following equation can be applied [40,44]:

$$\sigma = 2\sigma_{2D} \times h^2/\lambda_0,$$

$$(10)$$

where λ_0 is the wavelength of air at the operation frequency.

In the next section, we report the results of the numerical simulations carried out to optimize the cloak design and to identify the metasurface susceptibilities in realistic scenarios.

III. NUMERICAL RESULTS

As a study case, we consider a dipole antenna, featuring a radius of $a = 2$ mm and a length of $l = 43$ mm, resonating at a frequency of $f_0 = 3$ GHz. This antenna is surrounded by a bianisotropic metasurface with radius $a_c = 20$ mm. Such a radius, which corresponds to $\lambda_0/5$, represents a reasonable trade-off between the different requirements discussed at the end of the previous section.

Our investigation involves numerical simulations carried out using the metasurface model developed in accordance with the surface electric and magnetic currents, as detailed in Sec. II. We carried out two distinct simulations, one for transmission and another one for the scattering scenario. The desired cloaking performances are achieved by optimizing the susceptibilities of the metasurface. The optimal susceptibility values are determined to be $\chi_{ee}{}^{zz} = \chi_{em}{}^{z\varphi} = 0.04425 + 1.18i(m)$ and $\chi_{me}{}^{\varphi z} = \chi_{mm}{}^{\varphi\varphi} = 0.4 - 0.015i(m)$. As observed, $\chi_{em}{}^{z\varphi} \neq -\chi_{me}{}^{\varphi z}$ leads to the obvious conclusion that a bianisotropic nonreciprocal cloak is essential for our specific objectives.

The results shown in Fig. 2(a) obtained with finite-element-method-based simulations demonstrate a significant reduction of the in-band total scattering cross section (SCS) of the cloaked cylinder when surrounded by the designed bianisotropic nonreciprocal metasurface, compared to its uncloaked counterpart. Figure 2(b) shows the analytical results for the uncloaked and cloaked antennas. Although their behavior for analytical and numerical methods is completely identical, there is a shift in RCS
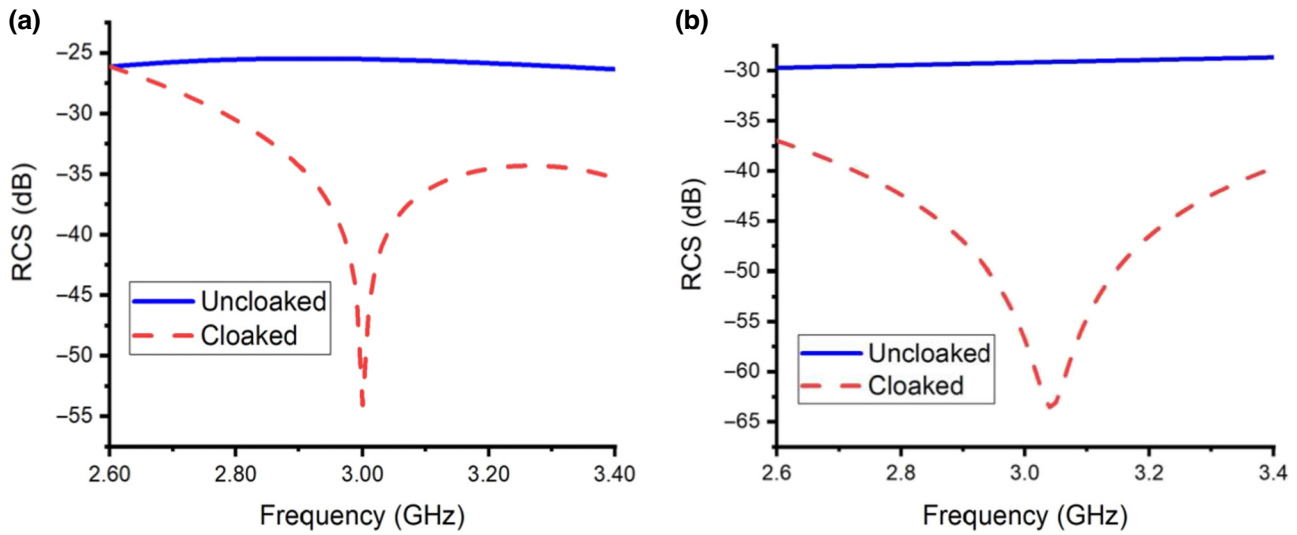
FIG. 2.   Scattering cross section versus the frequency of uncloaked and cloaked antennas in receiving mode: (a) simulation results; (b) analytical results.

levels due to the fact that we use the scattering-cancellation technique for a finite cylinder. Moreover, for an analytical solution, higher harmonics have been neglected. On the other hand, for radiation mode, Figs. 3 and 4 compare the polar plots on the vertical plane ($\phi = 90°$) and the 3D patterns of the realized gain of the cloaked and uncloaked antennas, respectively. As it can be appreciated, though the scattered power of the cloaked cylinder is significantly reduced, the realized gain of the antenna is relatively stable, as a result of metasurface nonreciprocity. Notably, a slight increase of the antenna realized gain is observed, which can be understood by considering the fact that the optimal susceptibilities obtained during optimization correspond to an active metasurface.

Having successfully optimized the performance of the cloak through the careful design of the bianisotropic nonreciprocal metasurface, in the next section, we introduce a feasible nonreciprocal metasurface design, facilitating the practical implementation of the cloak in real-world scenarios.

IV. IMPLEMENTATION OF THE NONRECIPROCAL CLOAK

Electromagnetic nonreciprocity can be achieved through different approaches, such as the use of anisotropic magnetic materials characterized by a nonsymmetric permeability tensor [45], the application of external magnetic fields to magnetoplasmonic metamaterials [46], the use of topological insulators [47], or time-reversal symmetry breaking [48].

Recent advancements have led to the creation of nonreciprocal metasurfaces by embedding unidirectional active circuit elements within the metal pattern [49]. Indeed, these elements behave as isolators and enable the flow

FIG. 3.   Polar plot of realized gain on the vertical plane ($\phi = 90°$) for uncloaked and cloaked antennas in transmitting mode.
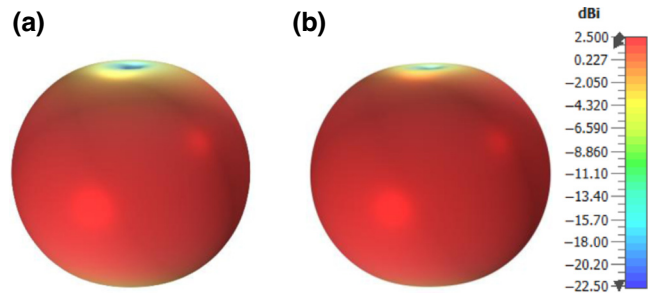

FIG. 4.   Comparison of 3D realized gain patterns for (a) uncloaked and (b) cloaked antennas.
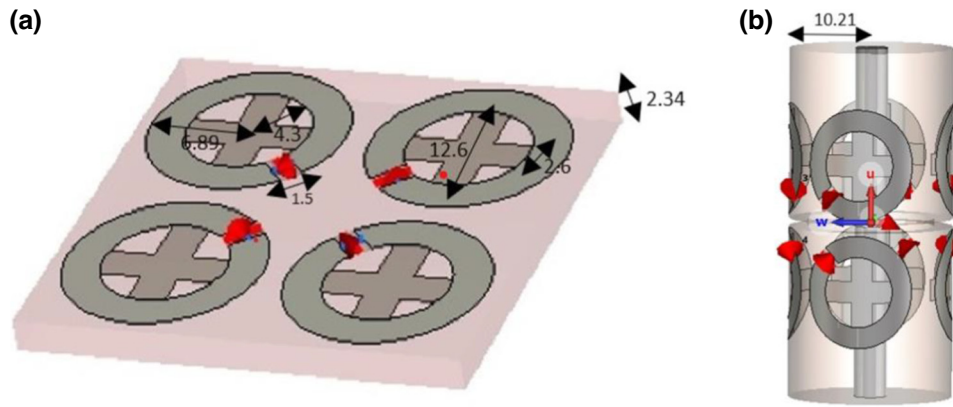
FIG. 5. Sketch of (a) designed nonreciprocal unit cell and (b) cloaked antenna. Sizes are expressed in mm. Red arrows in (a) show the physical location of isolators.

of the electric current in one direction only. Isolators can be effectively implemented using common field-effect transistors [50–52]. According to this approach, we have designed a bianisotropic nonreciprocal metasurface, the unit cell of which is depicted in Fig. 5(a). It consists of four split-ring resonators and cross dipoles arranged on a dielectric substrate [Arlon AD 430, with relative permittivity $\varepsilon_r = 4.3$ and loss tangent $\tan(\delta) = 0.003$] with periodicity equal to 31 mm. Isolators have been introduced within the slots to achieve nonreciprocal behavior. It is worth noting that, from a simulation point of view, the isolators are included in the unit cell through a set of circuital-electromagnetic cosimulations in the commercial software CST Studio Suite [53]. The geometrical size of the unit cell has been optimized through full-wave simulations to match the susceptibility values derived in the previous section. Figure 5(b) reports a sketch of the dipole antenna covered by the designed transparent cloak; the antenna is the same as that described in the previous section.

The total scattered power for both the uncloaked and cloaked antennas is shown in Fig. 6, while in Fig. 7 the corresponding 3D pattern is reported. These results confirm that, upon excitation of the cloaked cylinder by a TM_z-polarized plane wave, the cloaked antenna scatters a significantly lower power in comparison to its uncloaked counterpart because of the scattering-cancellation effect introduced by the transparent cloak. Another validation of the significant reduction in scattering from the cloaked antenna is provided in Fig. 8, wherein the electric field around the cloaked antenna for external illumination exhibits a plane-wave pattern, unlike the uncloaked antenna. Conversely, Figs. 9(a) and 9(c) show the radiation patterns of the bare and cloaked antennas, respectively. As expected, the antenna incorporating the transparent cloak exhibits a satisfactory radiation pattern that approaches the one of the original dipole without any cloak.

To demonstrate the effectiveness of the proposed nonreciprocal cloaking structure, we compare its performance

with that of a regular (reciprocal) mantle cloak. The reciprocal metasurface used for comparison consists of simple vertical strips and has been designed according to Ref. [9]. In Fig. 9(b), we show the realized-gain pattern of the half-wavelength dipole surrounded by the reciprocal metasurface. As can be appreciated, the radiation performance is quite poor, as a direct consequence of the constraints associated with the optical theorem.

Finally, Fig. 10 provides a comparison of the real and imaginary parts of the input impedance of the antenna when cloaked by nonreciprocal and reciprocal metasurfaces. The comparison reveals that the reciprocal cloak yields notably large values of the real and imaginary parts of the input impedance, resulting in poor total efficiency of the antenna. Conversely, in the case of the transparent cloak, these values closely align with the impedance of the
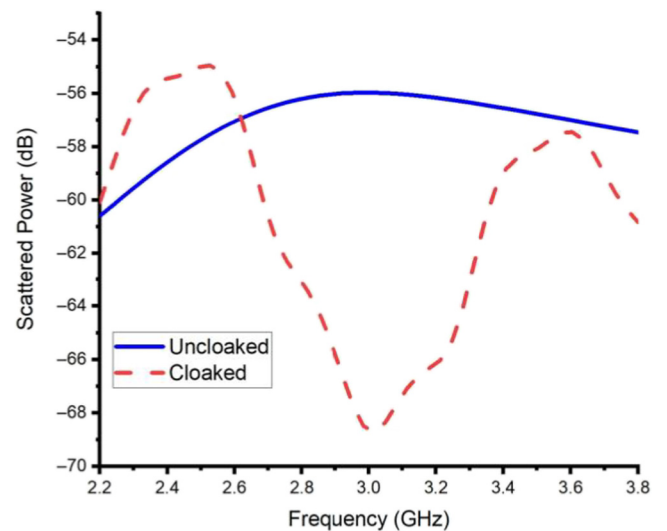

FIG. 6. Comparison of the total scattered power versus the frequency of uncloaked and cloaked antennas in the external illumination scenario.
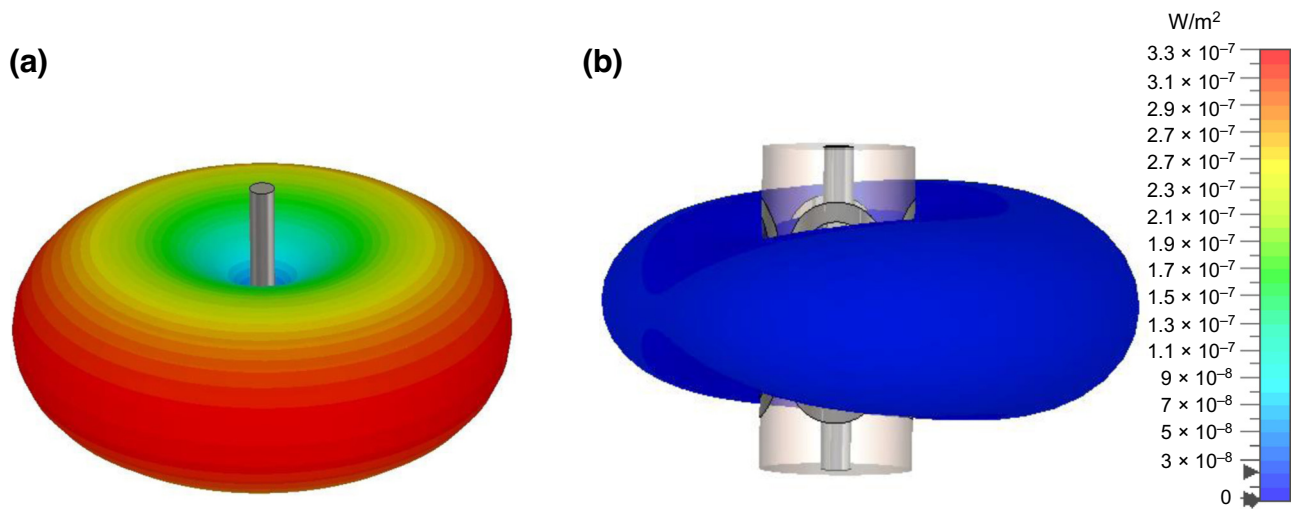
FIG. 7. Power scattering pattern of (a) uncloaked and (b) cloaked antennas in the external illumination scenario.
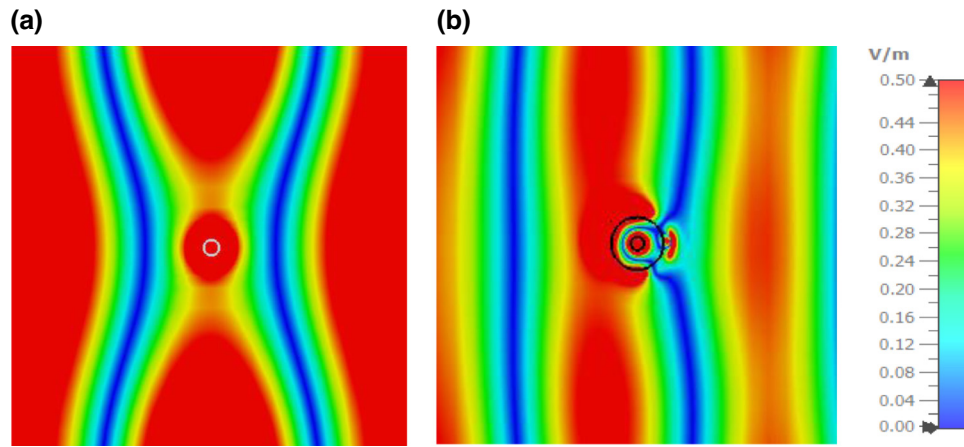

FIG. 8. Electric field distribution for (a) uncloaked and (b) cloaked antennas.
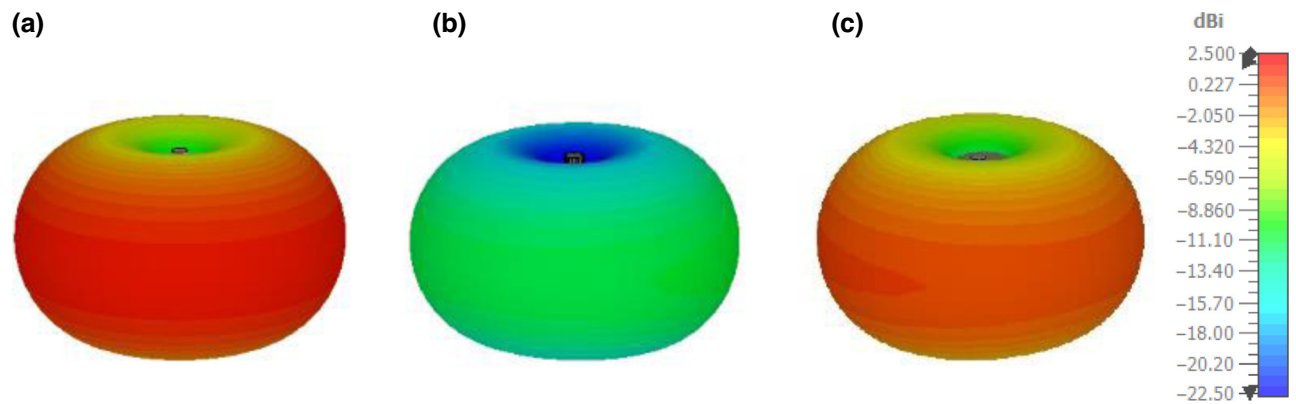

FIG. 9. Three-dimensional realized gain of (a) uncloaked, (b) reciprocally cloaked, and (c) nonreciprocally cloaked dipoles in the transmitting scenario.
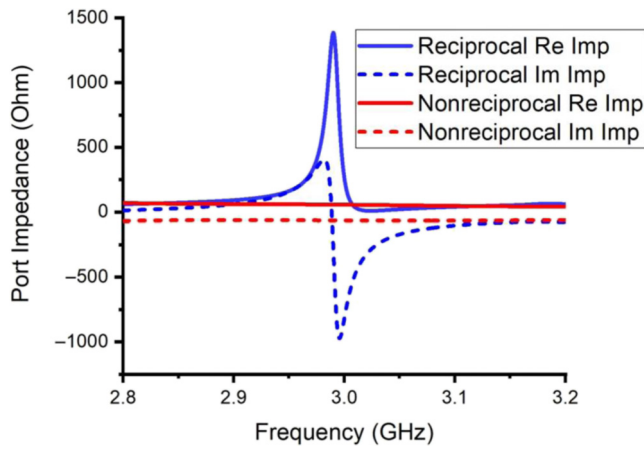
FIG. 10. Real and imaginary parts of the input impedance of the cloaked half-wavelength dipole. Two different scenarios are considered: antenna surrounded by a reciprocal cloak (blue lines) and a transparent nonreciprocal cloak (red lines).

bare dipole, allowing improved matching and increasing the realized gain of the antenna.

These results demonstrate the effectiveness of the nonreciprocal mantle cloak in rendering an antenna invisible at its own resonance frequency without compromising its radiation pattern, highlighting its potential for practical applications.

V. CONCLUSION

In this paper, we have put forward the concept of transparent mantle cloaks for antennas. Such innovative cloaks are realized through bianisotropic nonreciprocal metasurfaces and allow the fundamental limitations of passive cloaks to be overcome when used in combination with antennas. Specifically, we have presented a simple but effective theory to derive the metasurface susceptibilities and then designed a realistic transparent cloak based on an active metasurface layout. The results of numerical simulations confirm that the antenna cloaked with the active metasurface exhibits minimal scattering when exposed to an externally applied TM_z-polarized plane wave. At the same time, however, in transmission mode, the transparent cloak does not significantly affect the antenna performance, allowing operation of the antenna as if the cloak were not present. These results highlight the effectiveness of the proposed transparent cloak in achieving antenna invisibility, while preserving the radiation characteristics. We believe the proposed nonreciprocal cloak may find applications in different technical and scientific areas; for instance, they can be used to design antenna systems that can effectively communicate with the external world, without being detected by a detection system such as radar. Similarly, the suggested nonreciprocal cloak can be used

to mitigate mutual coupling between wire antennas operating at identical frequencies, which commonly occurs in phased array or multiple-input and multiple-output (MIMO) systems.

[1] C.A. Balanis, *Antenna Theory: Analysis and Design* (John Wiley & Sons, Hoboken, NJ, 2016).

[2] H. H. Sun, B. Jones, Y. J. Guo, and Y. H. Lee, Suppression of cross-band scattering in interleaved dual-band cellular base-station antenna arrays, IEEE Access **8**, 222486 (2020).

[3] J. Soric, Y. Ra'di, D. Farfan, and A. Alù, Radio-transparent dipole antenna based on a metasurface cloak, Nat. Commun. **13**, 1114 (2022).

[4] J. B. Pendry, D. Schurig, and D. R. Smith, Controlling electromagnetic fields, Science **312**, 1780 (2006).

[5] Z. H. Jiang, P. E. Sieber, L. Kang, and D. H. Werner, Restoring intrinsic properties of electromagnetic radiators using ultralightweight integrated metasurface cloaks, Adv. Funct. Mater. **25**, 4708 (2015).

[6] P. Alitalo, O. Luukkonen, L. Jylha, J. Venermo, and S. A. Tretyakov, Transmission-line networks cloaking objects from electromagnetic fields, IEEE Trans. Antennas Propag. **56**, 416 (2008).

[7] S. A. Tretyakov, P. Alitalo, O. Luukkonen, and C. Simovski, Broadband electromagnetic cloaking of long cylindrical objects, Phys. Rev. Lett. **103**, 103905 (2009).

[8] J. Vehmas, P. Alitalo, and S. A. Tretyakov, Transmission-line cloak as an antenna, IEEE Trans. Antenna Wireless Propag. Lett. **10,** 1594 (2011).

[9] A. Monti, J. Soric, A. Alù, A. Toscano, and F. Bilotti, Anisotropic mantle cloaks for TM and TE scattering reduction, IEEE Trans. Antennas Propag. **63,** 1775 (2015).

[10] J. Soric, A. Monti, A. Toscano, F. Bilotti, and A. Alù, Multiband and wideband bilayer mantle cloaks, IEEE Trans. Antennas Propag. **63,** 3235 (2015).

[11] Y. R. Padooru, A. B. Yakovlev, P. Y. Chen, and A. Alù, Analytical modeling of conformal mantle cloaks for cylindrical objects using subwavelength printed and slotted arrays, J. Appl. Phys. **112,** 034907 (2012).

[12] H. Younesiraad, Z. Hamzavi-Zarghani, and L. Matekovits, Invisibility utilizing Huygens' metasurface based on mantle cloak and scattering suppression phenomena, IEEE Trans. Antennas Propag. **69,** 5181 (2021).

[13] Y. R. Padooru, A. B. Yakovlev, P.-Y. Chen, and A. Alù, Line-source excitation of realistic conformal metasurface cloaks, J. Appl. Phys. **112,** 104902 (2012).

[14] A. Monti, J. Soric, A. Alu, F. Bilotti, A. Toscano, and L. Vegni, Overcoming mutual blockage between neighboring dipole antennas using a low-profile patterned metasurface, IEEE Antennas Wirel. Propag. Lett. **11,** 1414 (2012).

[15] A. Monti, J. Soric, M. Barbuto, D. Ramaccia, S. Vellucci, F. Trotta, A. Alù, A. Toscano, and F. Bilotti, Mantle cloaking for co-site radio-frequency antennas, Appl. Phys. Lett. **108,** 113502 (2016).

[16] J. C. Soric, A. Monti, A. Toscano, F. Bilotti, and A. Alù, Dual-polarized reduction of dipole antenna blockage using mantle cloaks, IEEE Trans. Antennas Propagat. **63,** 4827 (2015).

[17] H. M. Bernety and A. B. Yakovlev, Reduction of mutual coupling between neighboring strip dipole antennas using confocal elliptical metasurface cloaks, IEEE Trans. Antennas Propag. **63,** 1554 (2015).

[18] Gabriel Moreno, Alexander B. Yakovlev, Hossein Mehrpour Berneti, Douglas H. Werner, Hao Xin, Alessio Monti, Filiberto Bilotti, Andrea Alu, Wideband elliptical metasurface cloaks in printed antenna technology, IEEE Trans. Antennas Propag. **66,** 3512 (2018).

[19] A. Monti, J. Soric, A. Alù, A. Toscano, and F. Bilotti, Design of cloaked Yagi-Uda antennas, EPJ Appl. Metamater. **3,** 10 (2016).

[20] H. M. Bernety, A. B. Yakovlev, H. G. Skinner, S.-Y. Suh, and A. Alù, Decoupling and cloaking of interleaved phased antenna arrays using elliptical metasurfaces, IEEE Trans. Antennas Propag. **68,** 4997 (2020).

[21] C. A. Bohren and D. R. Huffman, *Absorption and Scattering of Light by Small Particles* (John Wiley & Sons, Hoboken, NJ, 2008).

[22] W. K. Kahn and H. Kurss, Minimum-scattering antennas, IEEE Trans. Antennas Propag. **13,** 671 (1965).

[23] J. C. Soric, R. Fleury, A. Monti, A. Toscano, F. Bilotti, and A. Alù, Controlling scattering and absorption with metamaterial covers, IEEE Trans. Antennas Propag. **62,** 4220 (2014).

[24] A. Alù, Mantle cloak: Invisibility induced by a surface, Phys. Rev. B. **80,** 245115 (2009).

[25] Pai-Yen Chen, Mohamed Farhat, Sébastien Guenneau, Stefan Enoch, Andrea Alù, Acoustic scattering cancellation via ultrathin pseudo-surface, Appl. Phys. Lett. **99,** 19 (2011).

[26] P. Y. Chen and A. Alù, Atomically thin surface cloak using graphene monolayers, ACS Nano **5,** 7 (2011).

[27] S. Vellucci, A. Monti, M. Barbuto, G. Oliveri, M. Salucci, A. Toscano, and F. Bilotti, On the use of non-linear metasurfaces for circumventing fundamental limits of mantle cloaking for antennas, IEEE Trans. Antennas Propag. **69,** 5048 (2021).

[28] A. Monti, M. Barbuto, A. Toscano, and F. Bilotti, Nonlinear mantle cloaking devices for power-dependent antenna arrays, IEEE Antennas Wirel. Propag. Lett. **16,** 1727 (2016).

[29] S. Vellucci, A. Monti, M. Barbuto, A. Toscano, and F. Bilotti, Waveform-selective mantle cloaks for intelligent antennas, IEEE Trans. Antennas Propag. **68,** 1717 (2019).

[30] P. Y. Chen, C. Argyropoulos, and A. Alù, Broadening the cloaking bandwidth with non-Foster metasurfaces, Phys. Rev. Lett. **111,** 233001 (2013).

[31] D. L. Sounas, R. Fleury, and A. Alú, Unidirectional cloaking based on metasurfaces with balanced loss and gain, Phys. Rev. Appl. **4,** 014005 (2015).

[32] A. Kord, D. L. Sounas, and A. Alù, Active microwave cloaking using parity-time-symmetric satellites, Phys. Rev. Appl. **10,** 054040 (2018).

[33] M. Dehmollaian, G. Lavigne, and C. Caloz, Transmittable non-reciprocal cloaking, Phys. Rev. Appl. **19,** 014051 (2023).

[34] K. Achouri and C. Caloz, *Electromagnetic Metasurfaces: Theory and Applications* (John Wiley & Sons, Hoboken, NJ, 2021).

[35] C. Caloz, A. Alù, S. Tretyakov, D. Sounas, K. Achouri, and Z.-L. Deck-Lèger, Electromagnetic nonreciprocity, Phys. Rev. Appl. **10,** 047001 (2018).

[36] M. Idemen and A. H. Serbest, Boundary conditions of the electromagnetic field, Electron. Lett. **13,** 704 (1987).

[37] E. F. Kuester, M. A. Mohamed, M. Piket-May, and C. L. Holloway, Averaged transition conditions for electromagnetic fields at a metafilm, IEEE Trans. Antennas Propag. **51,** 2641 (2003).

[38] K. Achouri, M. A. Salem, and C. Caloz, General metasurface synthesis based on susceptibility tensors, IEEE Trans. Antennas Propag. **63,** 2977 (2015).

[39] V. Popov, A. D. Rubio, V. Asadchy, S. Tcvetkova, F. Boust, S. Tretyakov, and S. N. Burokur, Omega-bianisotropic metasurface for converting a propagating wave into a surface wave, Phys. Rev. B **100,** 125103 (2019).

[40] C.A. Balanis, *Advanced Engineering Electromagnetics* (John Wiley & Sons, New York, 1989).

[41] P. Y. Chen and A. Alù, Mantle cloaking using thin patterned metasurfaces, Phys. Rev. B **84,** 205110 (2011).

[42] Z. Hamzavi-Zarghani, A. Yahaghi, and L. Matekovits, Dynamically tunable scattering manipulation of dielectric and conducting cylinders using nanostructured graphene metasurfaces, IEEE Access **7,** 15556 (2019).

[43] J. C. Soric, P. Y. Chen, A. Kerkhoff, D. Rainwater, K. Melin, and A. Alù, Demonstration of an ultralow profile cloak for scattering suppression of a finite-length rod in free space, New J. Phys. **15**, 033037 (2013).

[44] Z. Hamzavi-Zarghani, A. Yahaghi, and L. Matekovits, Electrically tunable mantle cloaking utilizing graphene metasurface for oblique incidence, AEU Int. J. Electron. Commun. **116**, 153080 (2020).

[45] A. Ashley and D. Psychogiou, Ferrite-based multiport circulators with rf co-designed bandpass filtering, IEEE Trans. Microwave Theory Tech. **71**, 2594 (2023).

[46] Jessie Yao Chin, Tobias Steinle, Thomas Wehlus, Daniel Dregely, Thomas Weiss, Vladimir I. Belotelov, Bernd Stritzker, and Harald Giessen, Nonreciprocal plasmonics enables giant enhancement of thin-film Faraday rotation, Nat. Commun. **4**, 1599 (2013).

[47] L. Lu, J. D. Joannopoulos, and M. Soljačić, Topological photonics, Nat. Photonics **8**, 821 (2014).

[48] S. Buddhiraju, A. Song, G. T. Papadaki, and S. Fan, Nonreciprocal metamaterial obeying time-reversal symmetry, Phys. Rev. Lett. **124**, 257403 (2020).

[49] T. Kodera, D. L. Sounas, and C. Caloz, Artificial Faraday rotation using a ring metamaterial structure without Static Magnetic Field, Appl. Phys. Lett. **99**, 031114 (2011).

[50] G. Lavigne and C. Caloz, Magnetless reflective gyrotropic spatial isolator metasurface, New J. Phys. **23**, 075006 (2021).

[51] G. Lavigne, T. Kodera, and C. Caloz, Metasurface magnetless specular isolator, Sci. Rep. **12**, 5652 (2022).

[52] Y. Ra'di and A. Grbic, Magnet-free nonreciprocal bianisotropic metasurfaces, Phys. Rev. B. **94**, 195432 (2016).

[53] CST Studio Suite, 2024 [Online]. Available: www.cst.com